Deep Learning-Based Uplink Transmit Power Estimation in 4G/5G Networks

Álvaro Ribas[1], Qunfei Sun[2], Shanshan Wang[3], Joe Wiart[3]

[1]Institut Polytechnique de Paris – alvaro.tona@ip-paris.fr
[2]LIPADE, Université Paris Cité – qunfei.sun@etu.u-paris.fr
[3]Chair C2M, LTCI, Télécom Paris, Institut Polytechnique de Paris – {firstname.surname}@telecom-paris.fr

Keywords: Deep Learning, Electromagnetic Field Exposure, Uplink Transmit Power

Abstract

In urban environments, regulation for radiofrequency electromagnetic field (RF-EMF) exposure limits the intensity of these fields in wireless communication links between a user (UE) and a base station (BS), for health purposes. Therefore, it is relevant to quantify the power emitted by a user over space in time. A comprehensive measurement and assessment of E-field levels by BSs in micro-environments in France has been done by [1]. To be able to predict such levels using publicly available data, the work [2] proposes a convolutional neural network (CNN) method using heatmaps from the physical environment and the radiation patterns of antennas. The present work proposes to combine heatmap images with measurements of downlink (DL) frequencies of BSs to estimate the uplink (UL) power transmit by a UE in a 4G/5G network, using a deep learning framework.

1 Introduction

The growth of wireless communication networks in urban environments has led to growing public and regulatory concern regarding radiofrequency electromagnetic field (RF-EMF) exposure. In the context of 4G/LTE and 5G networks, the uplink (UL) transmission – from the user equipment (UE) to the base station (BS) – is of particular relevance, as the emitting source is in direct proximity to the human body. The power transmitted by the UE is therefore a critical quantity to assess in the context of exposure evaluation. However, direct measurements of UL transmit power at scale remains challenging, as it requires dedicated equipment and significant field campaigns. Data-driven approaches, particularly with the use of machine learning, offer a compelling alternative by enabling power estimation from publicly available information and a limited number of measurements.

Previous works have done a comprehensive measurement of E-field levels emitted by base stations in certain micro-environments in France, retaining information about the average transmit power and throughput [1]. Besides, methods based on convolutional neural networks (CNNs) to predict E-field levels in urban environments using physical heatmaps and antenna radiation patterns have been explored in [2]. The present work extends them by combining environmental heatmaps with downlink frequency measurements from base stations to estimate the UL transmit power of a UE in a 4G and 5G network, using a multi-branch deep learning architecture. The goal of this approach is to combine these spatial features and measurements to known characteristics of the wireless network, such as the free space path loss and antenna radiation patterns, to enrich the features of each different scenario and thus obtain better results in the prediction.

The remainder of this paper is organized as follows. Section 2 describes the data acquisition and preprocessing pipeline, including the public datasets and field measurements used. Section 3 details the deep learning model, covering the image generation algorithm, propagation and antenna models, network architecture, and training procedure. Section 4 presents and discusses the results obtained. Section 5 concludes the work and highlights directions for future research.

2 Data treatment

2.1 Obtaining public data

The data used in this work has two types: the public data, obtained through the Cartoradio website made by “Agence Nationale des Fréquences” (ANFR), and the measurements performed by [1]. The front page of the website is presented in figure 1. The map format of the page allows the user to select the region where the data is extracted, which is important to limit the number of base stations and thus the size of the dataset. A part of the antenna locations obtained is shown on the left side of figure 2. Notice that the figure represents central Paris, where the largest portion of the dataset is concentrated, but other cities are also considered (for instance, Massy, Gif-sur-Yvette and Amiens). Their datasets were extracted individually and without intersection – no base station was in two different areas – and later concatenated into one single dataset, to avoid capturing base stations beyond the desired regions.

Several datasets are obtained on the download from the website, of which two are used. The first contains information about the location of the base stations, namely the support number and coordinates (latitude and longitude). The second contains the information about the antennas, i.e. the support number, the date of service start, the operator, the type of antenna and its dimension, the directivity and the azimuth, the height with respect to the ground, the type of service, the system, and the smallest and largest frequencies in the band (in MHz or GHz). Both categories are grouped through the support number, so the location of each antenna and their main characteristics are represented in a single tensor.

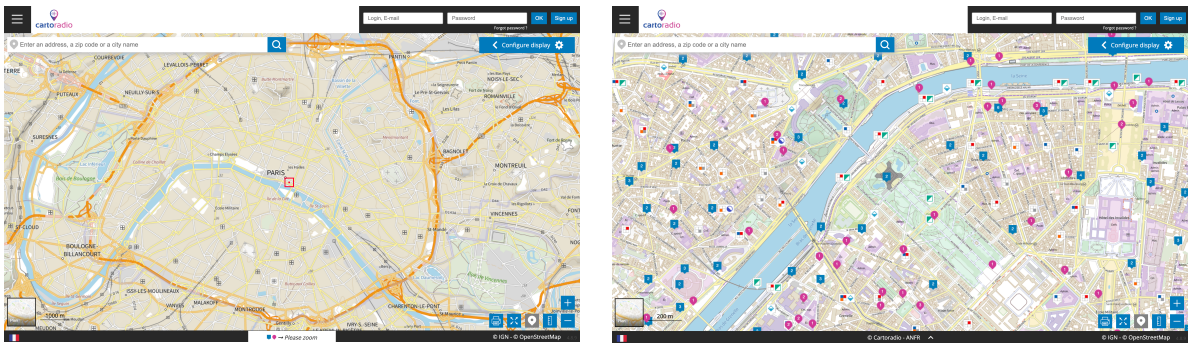

Figure 1: Main page of the Cartoradio website, where the region displayed is the center of Paris (left) and details of the antenna information around the Eiffel Tower region (right).

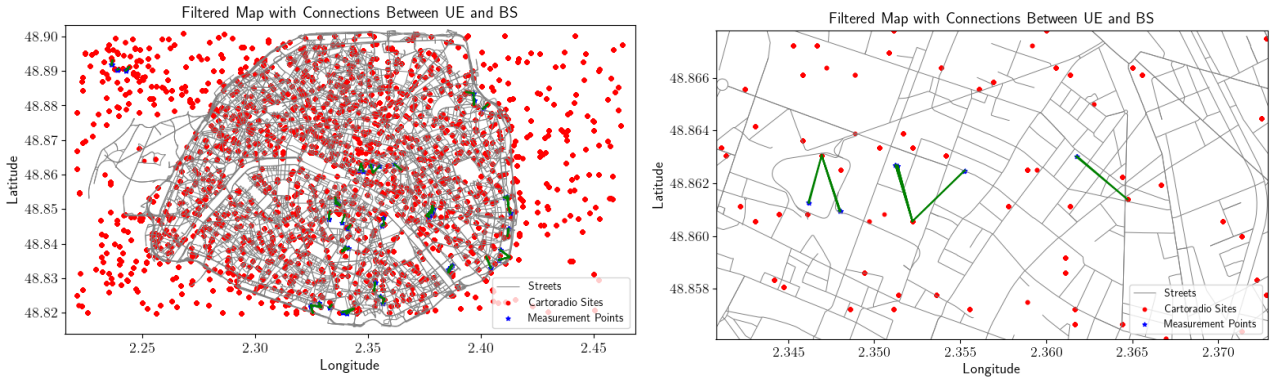

Figure 2: Plot of the base station locations obtained in central Paris, after filtering (left) and connections between UE and BS (right, in green). Details on filtering and BS selection are discussed in section 2.3.

2.2 Measurements using NEMO

For the second type of data, measurements of the connection between the user and the base station are performed using the NEMO Handy device by Keysight, an Android handheld solution that captures wireless diagnostics metrics. It captures information such as duration, packet technology, wireless technology, frequency band and transmit power for both the main and side links, energy, operator, and RSRP of primary and secondary cells.

Measurements are done in several locations. For each point, four types of application services are tested: FTP, voice call, video call, and VoIP. Naturally, this depends on availability, since not every location has a sufficiently strong connection to perform all of them, especially more data intensive protocols such as video calls. Consequently, the number of points is not the same for every location, but there is minimum of 1 and a maximum of 3 at each one. Furthermore, the coordinates of each point (latitude and longitude, in degrees) are registered manually in a separate file and later combined into the same tensor. The parameters are grouped through packet technology, frequency band and sidelink frequency band, i.e. each new value of these three criteria corresponds to a new line on the measurement's tensor.

2.3 Preprocessing pipeline

The two tensors, from Cartoradio and the measurements, are combined into one. To maintain the coherence in the data, so that every parameter measured finds an equivalence in the base stations, filtering and selection are needed. The criteria are independent from one another and thus could be done in any order, but, for simplicity, it is done the following way:

a. Beginning date of service: the measurements were done on 23/07/2023. Therefore, data from every base station installed after this date is disregarded.

b. Operator: despite several operators existing in France, the NEMO Handy only connects to base stations from Orange, Bouygues, SFR and Free. All other operators are disregarded.

c. Height of the antenna: some antennas are installed underground, whilst all measurements are done above ground level. All antennas with height $h \leq 0$ with respect to the ground are disregarded.

d. Downlink frequency: it's relevant to know the frequency band of operation for the uplink transmission of the UE, which implies selecting the downlink frequency of the BS. The selection is done according to the existing frequency band distribution in France, found in [3].

e. Environment: measurements are done either inside or outside buildings. Due to transmission loss effects (attenuation, fading, etc.), the received power in indoor measurements is subject to unknown environmental influence, which is not desired. Thus, only outdoor measurements are considered.

Beyond the filtering, there needs to be a selection on the connection between UE and BS. The criterium is a distance rank: a user is only connected to the physically nearest station that uses its same technology and operator. Therefore, even if the user is physically closer to one station, if it does not share the same operator or the same technology, the connection happens with another base station. This can be clearly observed on the right-hand side of figure 2.

Due to the scale of the city, the environment, and the distances between UE and BS, it's assumed that this criterium is equivalent to a power rank, i.e. the closest base station is also the one that provides the highest received power.

To calculate the distance between UE and BS, both the horizontal and vertical components are taken into consideration. It's assumed the UE is always at a height of 1.5 meters from the ground (on a tripod), and the height of the BS is in the height parameter of the Cartoradio tensor. The horizontal distance is calculated in kilometers, converted from degrees through the haversine distance – described in section 3.1. The true distance is a Euclidian combination of both. To find the closest BS to a user, a K-D tree nearest neighbor search algorithm is applied. The coordinates of the nearest base station found, as well as the distance (in kilometers), are inserted as new columns in the measurement's tensor.

The parameters of each of the final tensors are presented below in tables 1 and 2.

Parameter	Description
Beginning date of service	Used only for filtering out newer antennas
Operator	Defines compatibility criterium for K-D search
Azimuth	Provides the orientation of 4G/LTE antennas
Height of antenna	Direct input of the neural network
Type of service	Used only for filtering out services not read by the NEMO Handy
System	Defines compatibility criterium for K-D search
Band start	Minimum frequency of the band, direct input of the neural network
Band end	Maximum frequency of the band
Unit	MHz or GHz (for band start and end)
Latitude	Distance from the BS to the Greenwich [º]
Longitude	Distance from the BS to the Equator [º]

Table 1: Parameters retained in the Cartoradio tensor after processing.

Parameter	Description
Packet technology	Used only for matching data between measurement points
Band	Defines compatibility criterium for K-D search [MHz or GHz]
Sidelink band	Used only for matching data [MHz or GHz]
Transmit power	Ground truth for primary cell [mW]
Sidelink transmit power	Ground truth for secondary cell [mW]
File type	Direct input of the neural network
Operator	Defines compatibility criterium for K-D search
Latitude and longitude	Distances from UEs to Equator and Greenwich, respectively, [º]
Nearest latitude	Latitudinal distance to the nearest BS [º]
Nearest longitude	Longitudinal distance to the nearest BS [º]
Distance	Absolute value to the nearest BS [km], direct input of the neural network

Table 2: Parameters retained in the measurements tensor after processing.

3 Deep learning model

3.1 Algorithm to generate images

The representation of space on the surface of the Earth is done using coordinates, latitude and longitude, in degrees. However, due to the scale of the wireless links in this work, it's more convenient to make calculations in kilometers. The values in kilometers are later converted to pixels in the images, which shall be the same for both building images and antenna radiation images. This guarantees all images have the same dimensions and represent the same distance in the real world, which is essential to compare their features in the deep learning model (sections 3.3 and 3.4). The regions of interest are the 500x500 meters spaces centered on each UE. To calculate lengths within this region, the haversine h between two points is taken, considering a distance d between them, $R = 6371\ km$ the radius of the Earth,

$$h\left(\frac{d}{R}\right) = \sin^2\left(\frac{d}{2R}\right) \tag{1}$$

In terms of the coordinates $(\delta_{lat}, \delta_{lon})$ of any points 1 and 2 on the surface,

$$h\left(\frac{d}{R}\right) = h\left(\delta_{lat,2}, \delta_{lat,1}\right) + \cos\left(\delta_{lat,1}\right)\cos\left(\delta_{lat,2}\right) h\left(\delta_{lon,2} - \delta_{lon,1}\right) \tag{2}$$

Therefore, by isolating d from the equation above,

$$d = \mathcal{H}(\delta_{lat}, \delta_{lon}) = 2R \arcsin\left(\sqrt{h\left(\delta_{lat,2}, \delta_{lat,1}\right) + \cos\left(\delta_{lat,1}\right)\cos\left(\delta_{lat,2}\right) h\left(\delta_{lon,2} - \delta_{lon,1}\right)}\right) \tag{3}$$

which is the equation used to calculate the distance and convert degrees to kilometers.

A problem still arises on the conversion: kilometers and degrees are not related by the same proportionality constant due to Earth's shape. Since the Earth is an irregular ellipsoid, flatter around the poles, the latitude conversion is almost the same everywhere (around 111 km/º), but the longitude conversion becomes smaller further from the Equator (until it reaches 0º at the poles). Therefore, the haversine distance algorithm is adapted, calculating horizontal distances along latitude and longitude separately. Besides, due to the dimension of the region of interest with respect to the radius of the Earth, the lengths around the user are approximated by straight line. Thus, all distances are calculated either along the same longitude or latitude.

3.2 Propagation and antenna models

The algorithm described above is first used to capture images from the environment where the measurements happen. Particularly, the space is represented as a map of the buildings around the point, both their contours and heights. The maps are extracted with the public API for geocoding from "Géoplataforme", using the coordinates from the measurement point (UE) as a reference: the center of the image. Furthermore, each image is 256x256 pixels and corresponds to a real distance of 500x500 meters. Examples from the dataset created are in figure 3 below.

Figure 3: Examples of building height maps extracted, cropped using the calculated distance. Higher buildings are lighter, whereas the ground is dark.

Wireless communications are also subject to effects of propagation losses, that must be considered when determining the power attenuation of a signal. This attenuation is described by a free space path loss (FSPL) model, which shall be as generic as possible to avoid problems when training the neural network (namely underfitting or overfitting), while still being complete enough to describe the propagation. In this work, no assumptions are made about the building density in the urban environment.

Thus, the model chosen has the distance d (in meters) and the frequency f as inputs, such that

$$FSPL_{dB} = 20\log_{10}(d) + 20\log_{10}(f) + 20\log_{10}\left(\frac{4\pi}{c}\right) \tag{4}$$

Besides the propagation, each antenna has different radiation patterns, depending on its geometry and technology. Since the exact specifications needed to calculate each pattern are unknown, approximations are needed. The work in [2] uses the common $\cos^m(\theta)$ approximation, which is more suitable for situations where the technology used is not specified. However, the technologies in this work are known, and thus better approximations can be used.

For 4G/LTE antennas, the radiation pattern is represented by three cardioids, generally described by

$$r(\theta) = a(1 + \cos(\theta + \varphi)) \tag{5}$$

where $a = 1$, and $\varphi_3 = \varphi_2 + 120° = \varphi_1 + 240°$, and $\varphi_1$is the azimuth direction. For 5G antennas, the pattern follows a von Mises distribution,

$$r(\theta, \kappa, \mu) = \frac{\exp(\kappa\cos(\theta - \mu))}{2\pi I_0(\kappa)} \tag{6}$$

where $\kappa = 7$, I_0 is the modified Bessel function, and the parameter μ is such that the center of the beam points to the user. This is a feature of beamforming technology in 5G and, in this case, the azimuth is ignored. Besides, the von Mises distribution is normalized, to be in the same scale as the cardioid. The polar plots of these patterns are done in figures 4. They are used to generate the radiation pattern images in figure 5, which have the same dimensions as the building height images. To account for the difference in intensity between 4G and 5G technologies, the intensity of the 5G signal at the antenna is normalized in 1.5, whereas the intensity in 4G is 1. Both signals decay logarithmically with the distance, following equation (4).

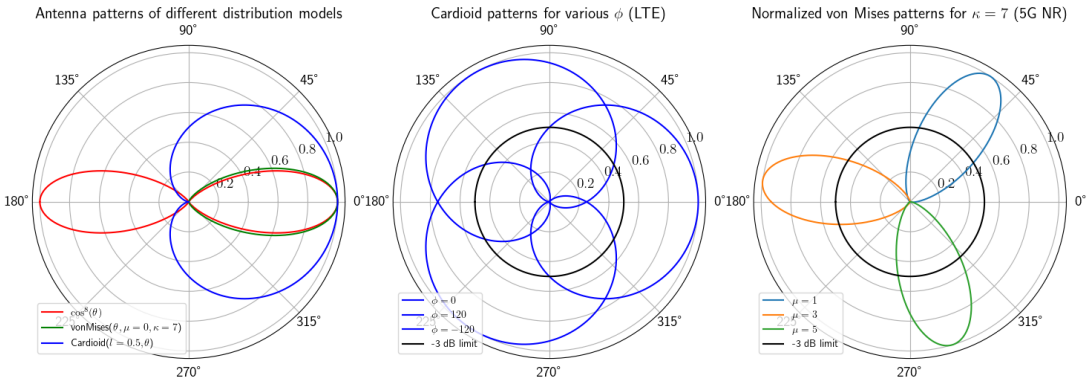

Figure 4: Candidates for antenna radiation pattern (left), cardioids chosen for 4G/LTE (center) and normalized von Mises chosen for 5G (right).

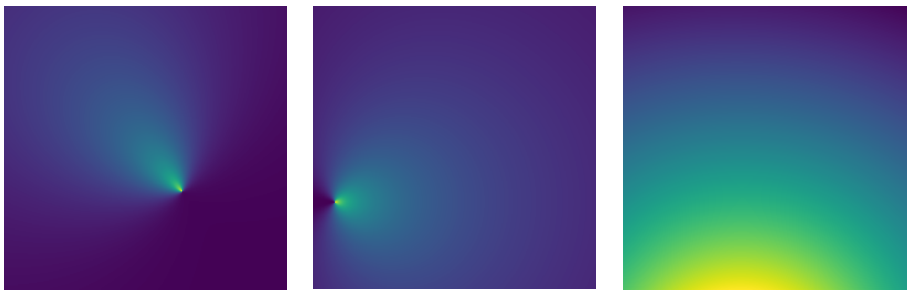

Figure 5: Examples of radiation pattern heatmaps for 4G (left, center) and 5G (right) technologies. Colors towards yellow represent a stronger signal, while towards indigo, a weaker signal.

3.3 Architecture

After preparing all data, the deep learning neural network architecture is now built. The main components of this network are the three branches (building, antenna, propagation), and three blocks (spatial fusion, frequency, and power). The global output is the value of the predicted uplink transmit power, at the power block. Its values are represented in a graph comparing the prediction to its ground truth, discussed in detail in section 4. Figure 6 below is an overview of the proposed architecture.

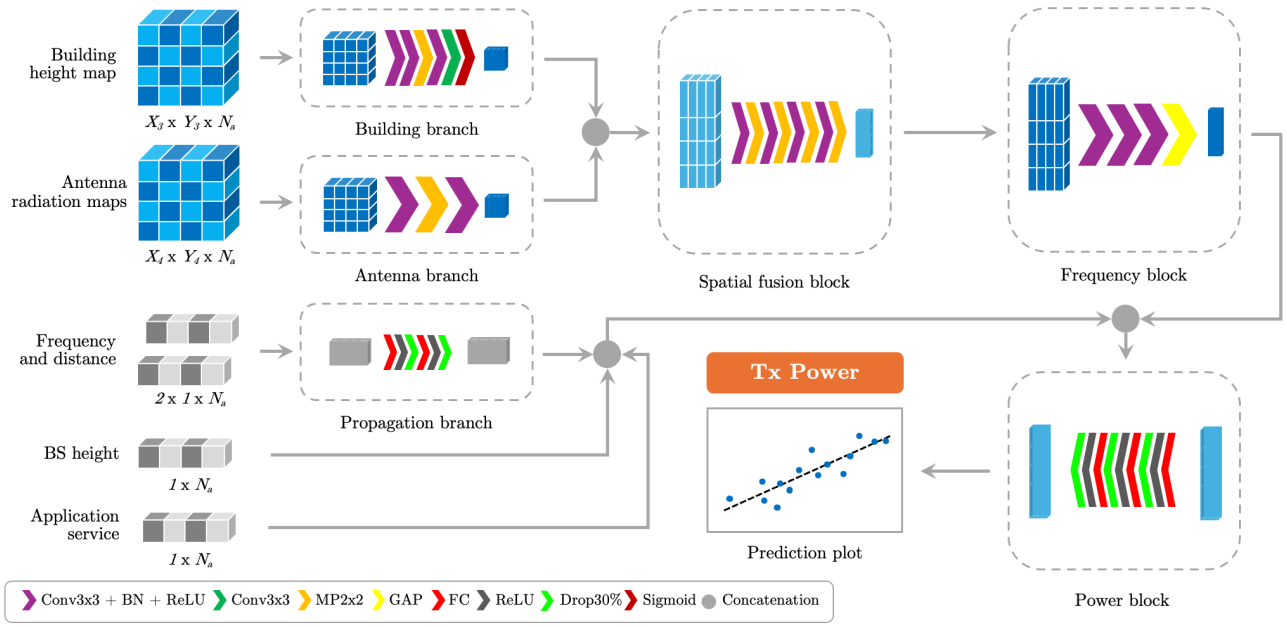

Figure 6: Architecture of the deep learning model. The operations performed within each block are described in the legend and detailed in section 3.3.1.

Building and antenna branches have as inputs the building height maps and antenna radiation maps, respectively. Their outputs are concatenated and processed by a spatial fusion block, which can retrieve spatial features from the images. Next, the output of the spatial fusion block is the input of the frequency block, where frequency-related features are extracted. In parallel, the propagation branch processes the frequency and distance information and relate through to equation (4). The result of this branch is concatenated both with the base station height information and the application service type, and later with the output of the frequency block, which becomes the input of the power block. The last step is to finally produce the predicted power and the associated graphs.

A brief description of how each main layer operates, and what is their general purpose in machine learning, can be found below in section 3.3.1.

3.3.1 Machine learning structures

a. 3x3 Convolutional Neural Network (CNN, Conv3x3): scans the image with a 3x3 kernel to detect simple patterns like edge and corners. A combination of these allows the model to extract complex spatial features (e.g., edges and textures) from the image.

b. Fully Connected (FC): a layer where each output neuron is connected to every input neuron, performing affine transformation to combine the learned features for prediction.

c. Batch Normalization (BN): standardizes activations per mini-batch to a range (typically [0,1]) with the goal of improving training stability, gradient flow, and convergence speed.

d. Max Pooling (MP): downsamples feature maps of the input by taking the maximum value in each local window, retaining salient responses and reducing spatial size.

e. Global Average Pooling (GAP): averages each feature map of the input over all spatial positions, producing a single value per channel and reducing parameters before classification.

f. ReLU and Sigmoid activation functions: non-linear functions used to limit the output range, address the influences of non-linearities in the model and mitigate problems such as vanishing gradients.

g. Dropout: regularization technique that randomly zeros a fraction of neurons in the network during the training phase to reduce co-adaptation and overfitting.

3.4 Training

The model is trained to predict transmission power from both images of building height and radiation patterns in single line tensors, such as frequency and distance. The target variable is originally provided in miliwatts (mW) and is converted

to dBm using $P_{dBm} = 10\log_{10}(P_{mW})$, so that the model learns in a logarithmic domain, which better reflects radio propagation behavior and stabilizes training across wide power ranges.

All column tensor inputs are standardized to zero mean and unit variance to improve optimization. The model outputs the transmit power directly in dBm, so no inverse conversion is needed during training. The loss function used is the Smooth L1 loss (or Huber loss), which is less sensitive to outliers than MSE and helps balance large and small errors. Optimization is performed with the Adam optimizer, including weight decay for regularization, and a "ReduceLROnPlateau" scheduler (with a fixed patience rate) that lowers the learning rate when validation performance stalls.

4 Results and discussion

The final predicted value obtained from the neural network is the transmit power. To verify the quality of the prediction, it is compared to its ground truth through a perfect prediction curve (where they are both equal). Then, the R^2 of the point distribution is calculated with respect to this curve, where results closer to 1 indicate a better relationship between them. The result is in figure 7.

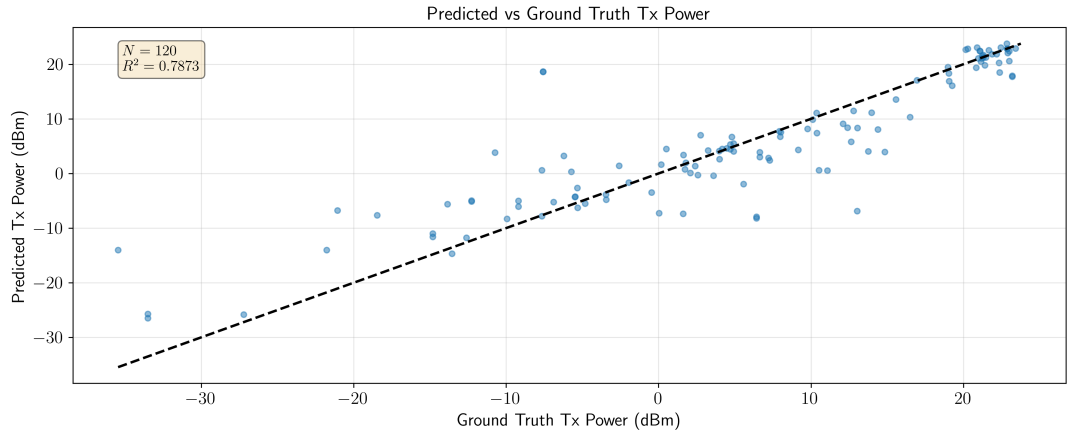

Figure 7: Results of the predicted transmit power compared to its ground truth in the test dataset. The black dotted line represents the ideal relationship.

Notably, there are only $N = 120$ points used for the fit, due to the split of the dataset between training (80%) and test/validation (20%), out of the $N_a = 603$ total points. The limitation in data points is a consequence of the reduced number of measurements that match the required criteria in filtering (section 2.3), particularly the "outdoor" requirement – many measurements were done indoors. Still, it is desired that the algorithm operates under limited data, since it's not convenient to make many real-world measurements due to the intrinsic difficulties in the campaign. A result of $R^2 = 0.7873$ is considered very adequate compared to the literature in [4].

Furthermore, a distribution of the error with respect to the perfect prediction is described through a histogram in figure 8 below. It calculates the vertical distance from each point to the perfect prediction line and shows how many points are within each range of 1 dB. For this histogram, a smaller standard error and a mean error closer to zero are equivalent to a better prediction.

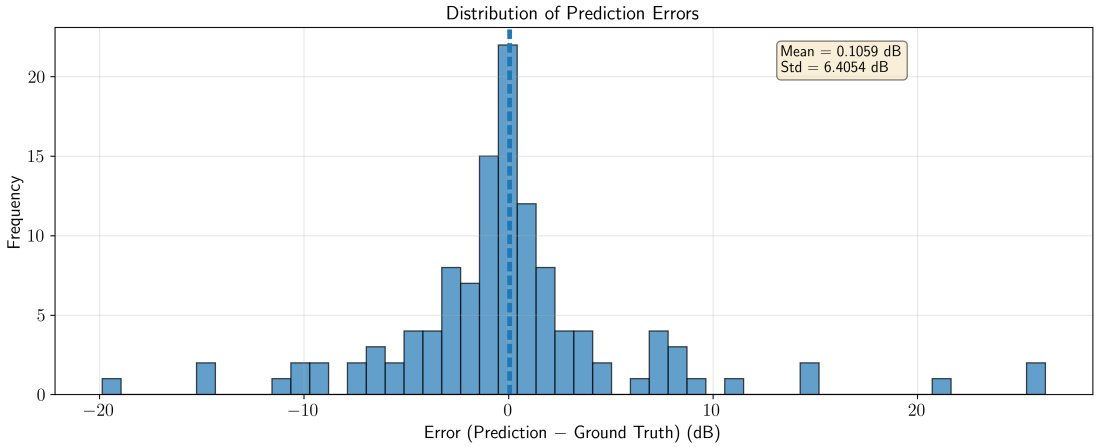

Figure 8: Distribution of transmit power prediction errors, in dB.

The figure shows that, despite the existence of outliers in the plot (notably around 25 dB and -15 dB), most points are still within a ±5 dB margin from the perfect prediction, and the standard deviation of the error is also around 6 dB, both of which are a positive indicator for the predictive performance of the neural network.

Finally, the quality of training can be observed through the Huber loss over the different epochs. If the training process is coherent, the loss should start at a high value from an initial guess and converge to a lower value as the epochs advance, until the error stabilizes. The training hyperparameters are shown in table 3, and the obtained loss graph is in figure 9.

Batch size	Number of epochs	Learning rate (LR)	Split ratio	LR reduction factor	Patience
12	250	0.001	0.80	0.5	15

Table 3: Hyperparameters of the best performance in training.

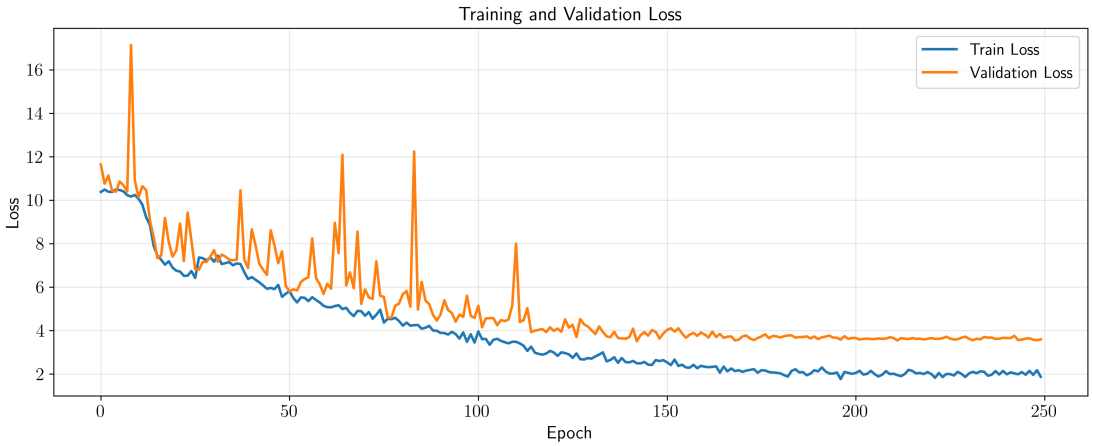

Figure 9: Huber loss per epoch throughout training epochs, both for training and testing/validation.

Given the two previous results, the convergence of the training is considered good, especially because it tends to a constant value after around 200 epochs for both train and validation sets.

5 Conclusion

This work proposed a deep learning-based approach to determine the uplink transmit power of a user equipment everywhere in an urban environment. The datasets used combined public data from ANFR with measurements from campaigns in the Paris region. Adequate filtering was done to make sure the data from both was compatible. There were considerations about the representation of the environment (buildings) around each measurement point, as well as the propagation losses and the antenna radiation pattern in each wireless link. A complete architecture had the most important parameters as inputs and was able to extract their features to make predictions. Due to the reduced size of the dataset after filtering, the prediction results with an $R^2 = 0.7873$ are considered promising. Future improvements shall revolve around ablation studies the architecture, applying a more concrete modelling to the propagation branch (the COST Hata model, for instance) or using measurements from other sites as test/validation sets.

6 Acknowledgments

This study was financed in part by the BRAFITEC program from “Coordenação de Aperfeiçoamento de Pessoal de Nível Superior” (CAPES) in Brazil, under Finance Code 001.

7 References

[1] J. Liu et al., *Assessment of EMF Exposure Induced by Wireless Cellular Phones in Various Usage Scenarios in France*, IEEE Access, vol. 13, pp. 123743-123755, 2025.

[2] Y. Zhang, S. Wang, J. Wiart, *ExposNet: A Deep Learning Framework for EMF Exposure Prediction in Complex Urban Environments*. 10.48550/arXiv.2503.02966.

[3] *Fréquences de téléphonie mobile en France*, Wikipedia, Wikimedia Foundation. Retrieved on December 2025.

[4] Q. Sun et al., *Measurement-Driven Deep Learning for Uplink RF Exposure Assessment in Urban Environments*. [Preprint]